Journal of Biomedical Optics

SPIEDigitalLibrary.org/jbo

Optical resolution photoacoustic microendoscopy with ultrasound-guided insertion and array system detection

Parsin Hajireza
Tyler Harrison
Alexander Forbrich
Roger Zemp

SPIE

Optical resolution photoacoustic microendoscopy with ultrasound-guided insertion and array system detection

Parsin Hajireza,* Tyler Harrison,* Alexander Forbrich, and Roger Zemp
University of Alberta, Department of Electrical and Computer Engineering, Edmonton, Alberta T6G 2V4, Canada

Abstract. Using a 0.8-mm-diameter image guide fiber bundle consisting of 30,000 single-mode fibers and an external linear array transducer, we demonstrate a dual-mode photoacoustic system capable of ultrasound-guided microendoscope insertion and photoacoustic imaging. The array optical resolution photoacoustic microendoscopy (AOR-PAME) system is designed to visualize the placement of the distal end of an endoscopy probe several centimeters into tissue, transmit scanning focused laser pulses into tissues via the fiber bundle, and acquire the generated photoacoustic signals. A ytterbium-doped fiber laser is tightly focused and is scanned across the proximal tip of the image guide fiber bundle using a two-dimensional galvanometer scanning mirror system. The end of the fiber bundle is used in contact mode with the object. The capabilities of AOR-PAME are demonstrated by imaging carbon fiber networks embedded in tissue-mimicking phantoms and the ears of a 60-g rat. The lateral resolution and signal-to-noise ratio are measured as 9 μm and 40 dB, respectively.
© *2013 Society of Photo-Optical Instrumentation Engineers (SPIE)* [DOI: 10.1117/1.JBO.18.9.090502]

Keywords: photoacoustic microscopy; endoscopy; optical resolution; array transducer; fiber optics; image guide; fiber laser.

Paper 130436LR received Jun. 27, 2013; revised manuscript received Aug. 21, 2013; accepted for publication Aug. 26, 2013; published online Sep. 25, 2013.

Photoacoustic microscopy (PAM) provides high-contrast images of tissues based on the physiological differences in the optical absorption of tissues.[1,2] Optically absorbing molecules absorb light, converting the energy into heat and causing thermoelastic expansion. This causes the emission of acoustic pressure waves detectable with an ultrasound transducer. Typical acoustic resolution PAM setups use loosely focused light and rely on the acoustic focal zone of the ultrasound transducer to achieve high-spatial resolution.[3] Optical resolution photoacoustic microscopy (OR-PAM), in contrast, uses scanned micron-scale focused light pulses to excite tissues, and lateral spatial resolution is defined by the optical rather than the acoustic focusing.[4] OR-PAM can be used for visualizing superficial capillary networks[5] and is also a powerful tool for quantifying functional parameters down to capillary sizes.[6] However, the shallow penetration depth of OR-PAM limits its application for clinical use.

Endoscopic imaging has enabled physicians to visualize the interior structures of the circulatory, respiratory, and digestive systems. Recently, our group introduced the capability of a label-free optical resolution photoacoustic microendoscopy (OR-PAME) system.[7,8] Ultrasound acquisition and light delivery are the two primary design challenges of an endoscopic OR-PAM system. Our previous OR-PAME systems take advantage of an image-guide fiber and a unique fiber laser with detection by a focused single-element ultrasound transducer. Extending the concept to real-world endoscopic applications using the previously reported OR-PAME system would be very challenging due to the difficulty in positioning of the external transducer.

One potential solution for the external transducer is to use all-optical detection techniques such as Fabry–Perot interferometry.[9] However, this solution will require another form of imaging to provide an external guidance of the endoscope. In this letter, we demonstrate a new version of OR-PAME using an ultrasound linear array transducer. Array-based optical resolution photoacoustic microendoscopy (AOR-PAME) offers several advantages over previous systems. First, photoacoustic acquisition and endoscope guidance use the same ultrasound transducer, reducing the required complexity of the setup. Second, positioning of the fiber can be aided with real-time B-mode ultrasound. Finally, delay-and-sum beamforming can be used to enhance the photoacoustic signals in the imaging plane by refocusing signals, meaning that fiber placement within the visual field of the array transducer does not need to be controlled precisely to capture an endoscopic image. This approach has the added benefit of being possible with a sufficiently fast ultrasound array system adapted for photoacoustic beamforming.[10]

In order to show the capabilities of AOR-PAME, carbon fiber networks and a rat's ear images are demonstrated. Using delay-and-sum beamforming, spatial resolution and signal-to-noise ratio (SNR) of the carbon fiber networks were measured as 9 μm and 40 dB, respectively. SNR is defined as the ratio of average signal in an area on the fiber to the standard deviation of an area off the fiber, in decibels, taken at a depth of ~2 cm. From previous photoacoustic work with the Verasonics array system, detection of ~5-cm deep within tissues is possible,[11] suggesting that this detection scheme is appropriate for OR-PAME systems for many locations in the body. Additionally, we demonstrate fiber guidance and endoscopic image capture through the tissue-mimicking phantom using only hand guidance. Thus, we believe that the AOR-PAME system can be used in future clinical applications.

The basic experimental setup is shown in Fig. 1. A 532-nm diode-pumped ytterbium fiber laser (YPL-G, IPG Photonics Corporation, Oxford, Massachusetts) with 1-ns pulse width, up to 600-kHz pulse repetition rate, and energy up to 20 μJ is coupled into a single-mode fiber, collimated, and then directed into a two-dimensional scanning mirror system (6203H, Cambridge Technology Inc., Bedford, Massachusetts). The mirrors are controlled by a two-channel function generator (AFG3022B, Tektronix Inc., Beaverton, Oregon). For our experiments, a laser pulse repetition rate of 20 kHz and energy

*These authors contributed equally.

Address all correspondence to: Roger Zemp, University of Alberta, Department of Electrical and Computer Engineering, Edmonton, Alberta, Canada. Tel: (780) 492-1825; Fax: (780) 492-1811; E-mail: rzemp@ualberta.ca

0091-3286/2013/$25.00 © 2013 SPIE

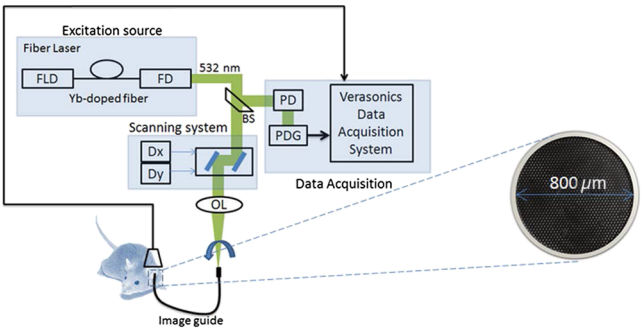

Fig. 1 Experimental setup of array optical resolution photoacoustic microendoscopy (AOR-PAME). FLD, fiber laser driver; Yb, ytterbium; FD, frequency doubling; BS, beam splitter; PD, photodiode; DX, *X* axis mirror driver; DY, *Y* axis mirror driver; OL, objective lens; PDG, pulse delay generator.

of 500 nJ is used. The frequency of the fast and slow mirrors is fixed at 5 and 0.05 Hz, respectively. The light from the mirrors is focused by an objective lens ($f = 4$ mm, 518125, LEICA, Germany) into the input end of the image guide fiber, consisting of 30,000 individual fibers in a 0.8-mm bundle. In order to trigger the ultrasound acquisition system, a beam splitter is used to pick off a part of the beam and redirect it into a photodiode. The photodiode signal is run through a delay generator (SRS-DG645), which is used to downsample to 1 kHz and delay the signal by almost one cycle to account for the speed constraints and triggering delay in the ultrasound acquisition system.

The ultrasound signals are collected by an L7-4 linear array transducer connected to a Verasonics VDAS ultrasound acquisition system. This captures data at a rate of 20 Msamples/s across all 128 elements simultaneously at 1000 fps and a depth of ~1500 samples. Due to memory constraints, we are only capable of capturing data for 10,000 points. Data are processed postcapture on a host PC to produce focused images for each of the 10,000 points and then a maximum amplitude projection is taken to produce a final image. Since we are using sinusoidal scanning, the image is reinterpolated on a square grid. The feedback signals used for the reinterpolation are simulated based on the function generator parameters to simplify data collection. After interpolation to the 100×100 square grid, a 3×3 Gaussian filter is applied with $\sigma = 0.5$ to provide some smoothing of honeycomb noise associated with the image guide structure and laser pulse positional uncertainty, and images are shown on a linear color scale.

Tissue-mimicking phantoms were formed using 10% w/v of both porcine gelatin and corn starch. This is a tissue-mimicking phantom commonly used in photoacoustic imaging studies that provides similar optical and acoustic properties to human tissue. The phantom was formed in a mold, and a hole was formed using an appropriately sized drill bit. Carbon fibers were pushed to the bottom of this hole, and water was used to fill the hole for acoustic coupling. The image guide was then threaded down the hole using ultrasound imaging for guidance and then an endoscopic image was captured. During this whole process, both the image guide and array transducer were held by hand with no additional stabilization, unlike our previous experiments.[12] Additionally, the connector was removed from the end of the image guide, allowing the hole that the endoscope was guided through to be much smaller than in previous experiments. This experiment shows the practicality of the proposed AOR-PAME.

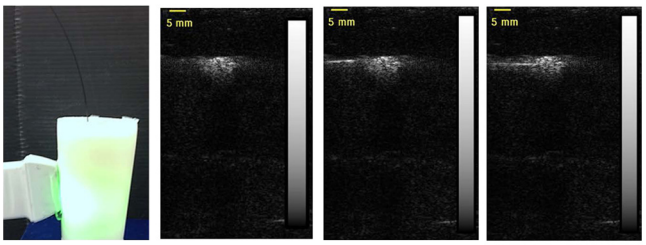

Fig. 2 (a) Phantom setup with ultrasound images of (b) before (Video 1), (c) during (Video 1) and (d) after insertion of endoscope (Video 1, MOV, 0.8 MB) [URL: http://dx.doi.org/10.1117/1.JBO.18.9.090502.1]. (b)–(d) are rotated 90 deg counterclockwise in comparison to (a).

For *in vivo* studies, we imaged the ears of a 60-g rat. All the experimental procedures were carried out in conformity with the laboratory animal protocol approved by the University of Alberta Animal Use and Care Committee. Authors are also trained and certified in order to use rats in the research work. During the imaging session, the animal was anesthetized with isoflurane using a breathing anesthesia system (E-Z Anesthesia, Euthanex Corp., Palmer, Pennsylvania).

Figure 2 shows the phantom imaging setup as well as images of the tunnel as the fiber is being inserted. After the fiber was guided to the embedded carbon fibers, several images were taken as shown in Fig. 3. SNR is measured at ~40 dB in spite of the ~2 cm of ultrasound attenuation through the tissue phantom.

Figure 4 shows blood vessels of the ear of a 60-g rat. The *in vivo* image of the ear was very challenging to capture due to the pressure exerted on the ear by the fiber that was necessary

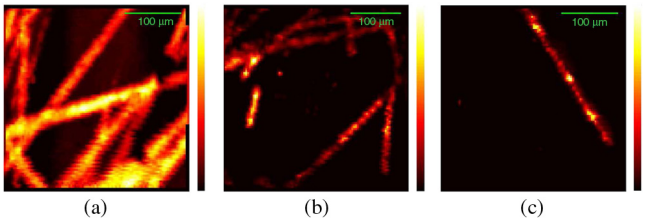

Fig. 3 Carbon fiber images captured from ~2-cm depth in tissue-mimicking phantom, (a) and (b) show fiber networks, (c) shows a single carbon fiber. SNR is ~40 dB, best-case resolution ~9 μm.

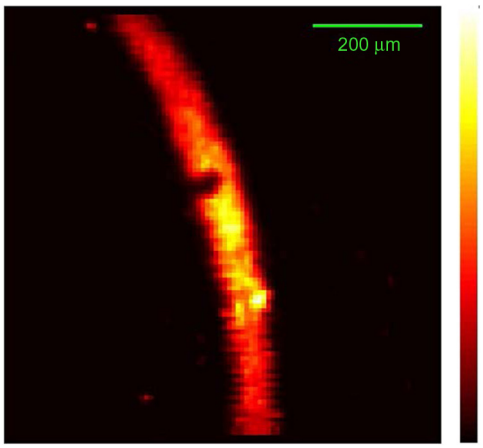

Fig. 4 *In vivo* AOR-PAM image of a rat's ear.

to ensure contact, which tended to drive blood out of the tissue. Using a GRIN lens at the tip of the fiber can solve this problem by removing the requirement for contact, with a trade-off having a larger footprint.[8] Improved means of mitigating pressure-induced flow blockage should be investigated in future work. Future clinical applications could include imaging colorectal and gastrointestinal cancers and dysplasia. *In vivo* endoscopic applications can be investigated in the future.

The full-width half-maximum of a single-carbon fiber was measured as ~11 μm in Fig. 3, which corresponds to ~9 μm based on convolution measurements.[13] Although it is possible to form images from the raw data, there are significant advantages in terms of SNR using beamforming: our previous work has shown a 21-dB increase.[12] Currently, delay-and-sum beamforming is performed on the entire image for all 10,000 photoacoustic events (each with 128 channels and 1500 samples per channel) which takes ~3 min to complete. However, by limiting the acoustically beamformed region to an area around the fiber tip and using fixed-focus delay and sum, reconstruction could be sped up to real-time, since current reconstruction forms an entire acoustically focused photoacoustic image for each optically focused point. The current SNR is promising for detection deep in tissue (~5 cm). However, if necessary, the SNR could be improved by averaging the raw photoacoustic data of multiple images before beamforming. We believe that AOR-PAME, with capabilities of image guidance and deep capture, may have a significant impact on emerging endoscopic applications.

In vivo clinical endoscopic applications can be investigated in the future, such as colorectal and gastrointestinal cancers and dysplasia imaging. In summary, array-based OR-PAME with the capabilities of external guidance of the endoscope tip and the data capture has been demonstrated. Both the ultrasound transducer and the endoscope were held and guided by hand. The entire footprint of the endoscopy tip was ~1 mm. The images of carbon fiber networks and *in vivo* imaging were demonstrated. The SNR in the phantom study was measured as ~40 dB through 2 cm of tissue-mimicking phantom material. Based on the previous work, we believe that it should be possible to push the endoscope depth to ~5 cm or more though SNR may be lower which may be mitigated by averaging multiple images. Photoacoustic endoscopy has significant potential for investigating cancer and other diseases, and array-based photoacoustic detection is a simple way to minimize the footprint of the endoscope allowing for greater system flexibility.

Acknowledgments

We gratefully acknowledge funding from Killam Trust for an Izaak Walton Killam Memorial Scholarship and Alberta Innovates, Technology Futures and Alberta Enterprise and Advanced Education for Graduate Student Scholarships and an SPIE Scholarship in Optics & Photonics. We also gratefully acknowledge funding from NSERC (355544-2008, 375340-2009, STPGP 396444), Terry-Fox Foundation and the Canadian Cancer Society (TFF 019237, TFF 019240, CCS 2011-700718), the Alberta Cancer Research Institute (ACB 23728), the Canada Foundation for Innovation, Leaders Opportunity Fund (18472), Alberta Advanced Education & Technology, Small Equipment Grants Program (URSI09007SEG), Microsystems Technology Research Initiative (MSTRI RES0003166), University of Alberta Startup Funds, and NSERC student scholarships.

References

1. P. Hajireza, A. Forbrich, and R. J. Zemp, "Multifocus optical-resolution photoacoustic microscopy using stimulated Raman scattering and chromatic aberration," *Opt. Lett.* **38**(15), 2711–2713 (2013).
2. G. Li, K. I. Maslov, and L. V. Wang "Reflection-mode multifocal optical-resolution photoacoustic microscopy," *J. Biomed. Opt.* **18**(3), 030501 (2013).
3. K. Maslov et al., "Optical-resolution photoacoustic microscopy for in vivo imaging of single capillaries," *Opt. Lett.* **33**(9), 929–931 (2008).
4. P. Hajireza, W. Shi, and R. J. Zemp, "Real-time handheld optical-resolution photoacoustic microscopy," *Opt. Express* **19**(21), 20097–20102 (2011).
5. S. Hu et al., "Functional transcranial brain imaging by optical-resolution photoacoustic microscopy" *J. Biomed. Opt.* **14**(4), 040503 (2009).
6. J. Chen et al., "Blind-deconvolution optical-resolution photoacoustic microscopy in vivo," *Opt. Express* **21**(6), 7316–7327 (2013).
7. P. Hajireza, W. Shi, and R. J. Zemp, "Label-free in vivo fiber-based optical-resolution photoacoustic microscopy," *Opt. Lett.* **36**(20), 4107–4109 (2011).
8. P. Hajireza, W. Shi, and R. Zemp, "Label-free in vivo GRIN-lens optical resolution photoacoustic micro-endoscopy," *Laser Phys. Lett.* **10**(5) 055603 (2013).
9. P. Hajireza et al., "Glancing angle deposited nanostructured film Fabry-Perot etalons for optical detection of ultrasound," *Opt. Express* **21**(5), 6391–6400 (2013).
10. T. Harrison and R. J. Zemp, "The applicability of ultrasound dynamic receive beamformers to photoacoustic imaging," *IEEE Trans. Ultrason. Ferroelectrics Freq. Control* **58**(10), 2259–2263 (2011).
11. T. Harrison and R. J. Zemp "Coregistered photoacoustic-ultrasound imaging applied to brachytherapy," *J. Biomed. Opt.* **16**(8), 080502 (2011).
12. T. Harrison et al., "Optical-resolution photoacoustic micro-endoscopy with ultrasound array system detection," *Proc. SPIE* **8581**, 85810C (2013).
13. W. Shi et al., "Optical resolution photoacoustic microscopy using novel high-repetition-rate passively Q-switched microchip and fiber lasers," *J. Biomed. Opt.* **15**(5), 056017 (2010).